

# Observation of the Imidazole-Imidazolium Hydrogen Bonds Responsible for Selective Proton Conductance in the Influenza A M2 Channel

Riqiang Fu,\* Yimin Miao, Huajun Qin, and Timothy A. Cross

Cite This: *J. Am. Chem. Soc.* 2020, 142, 2115–2119

Read Online

ACCESS |

Metrics & More

Article Recommendations

Supporting Information

**ABSTRACT:** The integral membrane M2 protein is a 97-residue membrane protein that assembles as a tetramer to conduct protons at a slow rate ( $10^2$ – $10^3$ /s) when activated by low pH. The proton conductance mechanism has been extensively debated in the literature, but it is accepted that the proton conductance is facilitated by hydrogen bonds involving the His37 residues. However, the hydrogen bonding partnership remains unresolved. Here, we report on the measurement of  $^{15}\text{N}$ – $^{15}\text{N}$   $J$ -couplings of  $^{15}\text{N}$  His37-labeled full length M2 (M2FL) protein from *Influenza A* virus embedded in synthetic liquid crystalline lipid bilayers using two-dimensional  $J$ -resolved NMR spectroscopy. We experimentally observed the hydrogen-bond mediated  $J$ -couplings between  $\text{N}_{\delta 1}$  and  $\text{N}_{\epsilon 2}$  of adjacent His37 imidazole rings, providing direct evidence for the existence of various imidazolium-imidazole hydrogen-bonding geometries in the histidine tetrad at low pH, thus validating the proton conduction mechanism in the M2FL protein by which the proton is transferred through the breaking and reforming of the hydrogen bonds between pairs of His37 residues.

The M2 protein from the *Influenza A* virus is a 97-residue membrane protein with a 24-residue N-terminal and a 51-residue C-terminal segment connected by a single transmembrane (TM) helix of 22 residues. It assembles as a tetrameric bundle to form a channel that is activated at low pH to conduct protons at a slow rate ( $10^2$ – $10^3$ /s), essential for the viral life cycle.<sup>1,2</sup> The  $\alpha$ -helical TM domain (residues 25–46) is responsible for proton conductance triggering the release of viral RNA into the host cells. This tetrameric TM domain is an important drug target.<sup>3–6</sup> The four His37 residues reside near the center of the TM helix and are known to be the heart of the proton conducting channel, the key to the proton transport mechanism.<sup>7</sup> Several different constructs reconstituted in various lipid environments have been the subject of intensive high-resolution structural studies in the past decade using both magic-angle-spinning (MAS)<sup>8–15</sup> and oriented sample<sup>3,16–19</sup> solid-state NMR, as well as solution NMR<sup>20–23</sup> and X-ray crystallography.<sup>24,25</sup> It has been clear so far that the proton conductance in the M2 channel is facilitated through hydrogen bonds with the His37 residues. But two possible models for His37 hydrogen bonding partners have been presented and debated in the literature (Figure 1) that form low-barrier hydrogen bonds (LBHB) as previously suggested with  $^1\text{H}$  frequencies as high as 18.7 ppm and protonated  $^{15}\text{N}$  frequencies as high as 195 ppm; i.e., the proton is transferred through protonating the  $\tau$  state of one His-His<sup>+</sup> pair to form a +3 state for the His tetrad prior to deprotonation and reforming the +2 state of the His tetrad.<sup>7,17,26</sup> If the His37 residue does not form His-His hydrogen bonded pairs, but only hydrogen bonds with water (cf. Figure 1b), a proton shuttling mechanism is proposed; i.e., the His37 shuttles protons through imidazole ring reorientations and exchanging protons with water.

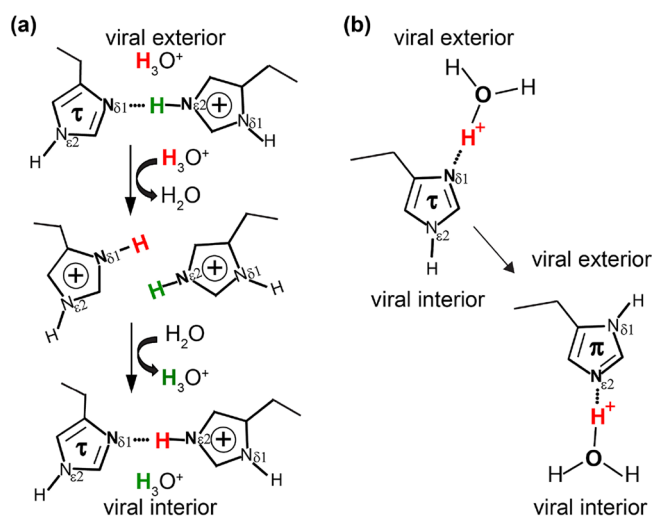


**Figure 1.** Two possible hydrogen bonding partnerships in the His37 tetrad of the M2 proton channel. (a) One of two pairs of His37 residues showing the low-barrier hydrogen bond model, in which the proton is transferred through the breaking and reforming of the intermonomer imidazole-imidazolium hydrogen bonds between His37 residues; (b) the water-His37 hydrogen bonding model, in which the His37 shuttles protons through imidazole ring reorientations and exchanging protons with water.

Received: September 15, 2019

Published: January 23, 2020

tions and exchanging protons with water without forming an intermonomer hydrogen bond between the His37 residues.<sup>27–29</sup>

To support the shuttling mechanism, two-dimensional (2D)  $^1\text{H}$ – $^{15}\text{N}$  heteronuclear correlation (HETCOR) experiments were performed to see if there were any correlations between the water protons and the nitrogens in the His37 side chains. It has been shown in the  $^1\text{H}$ – $^{15}\text{N}$  HETCOR spectra<sup>28</sup> of an M2 transmembrane construct, M2(22–46), in a virus-envelope-mimetic lipid membrane that the  $^{15}\text{N}$  peaks were in the range 160–180 ppm, correlating to  $^1\text{H}$  chemical shifts of 8–12 ppm, similar to a typical backbone amide  $^1\text{H}$  chemical shift range, and correlating to the  $^1\text{H}$  peak of water at  $\sim 5$  ppm. No imidazole-imidazolium cross peaks were observed in the  $^{13}\text{C}$ – $^{13}\text{C}$  correlation spectra of the +2 charged state of M2(22–46).<sup>27</sup> However, the correlated peaks between  $^{15}\text{N}$  and water protons can arise either from direct water-His proton transfer (cf. Figure 1b) or from additional protonation to form a transient +3 state for the His tetrad prior to deprotonation, potentially from a water in the viral interior (i.e., indirect transfer through the chemical exchange between hydronium ions and the protons of the histidine side chain NH bonds),<sup>26</sup> as illustrated in Figure 1a. Recently, more experimental evidence has been obtained as alluded to above from the full length M2 (M2FL) protein in lipid bilayers that support the LBHB model: (i) both high  $^1\text{H}$  and  $^{15}\text{N}$  frequencies extend up to 19 and 190 ppm, respectively, in the 2D  $^1\text{H}$ – $^{15}\text{N}$  HETCOR spectra, and the nonprotonated  $^{15}\text{N}$  resonances extending from 250 ppm down to 235 ppm—such extreme frequencies clearly indicate the formation of short imidazole-imidazolium hydrogen bonds in the His37 tetrad;<sup>26,30</sup> (ii) the observation that the hydronium ions are in chemical exchange on a subsec time scale with the protons of the imidazole-imidazolium hydrogen bonds;<sup>31</sup> (iii) the observations of  $^{13}\text{C}$ – $^{13}\text{C}$  and  $^{15}\text{N}$ – $^{15}\text{N}$  chemically exchange cross peaks between His37 residues in the neutral and charged states;<sup>32</sup> and (iv) no evidence for the  $\pi$  state under even mild acidic pH conditions when characterizing the full length protein.<sup>26</sup> Nevertheless, these results may still be considered as indirect evidence to affirm the LBHB model. Here, we seek direct and definitive evidence for the imidazole-imidazolium hydrogen bonding partner by measuring through-bond scalar coupling, i.e.  $J$ -coupling, between the two nitrogen sites.

A hydrogen bond is primarily an electrostatic attraction between two polar groups containing highly electronegative atoms such as nitrogen, oxygen, and fluorine that are bridged by a hydrogen atom. However, charge transfer (covalency) and dispersive energies are also important, especially when considering strong hydrogen bonds.<sup>33</sup> It has been well-known that the electron sharing within covalent bonds results in  $J$ -couplings. Similarly, the redistribution of electron densities upon hydrogen bond formation acts as electron sharing between the two nuclei involved in the hydrogen bond, although they are not covalently bonded.<sup>34</sup> As a result, there exist hydrogen-bond mediated  $J$ -couplings between the two electronegative atoms involved.<sup>35</sup> Such  $J$ -couplings across the hydrogen bonds have been observed in both solution<sup>36–40</sup> and solid-state NMR<sup>41–43</sup> spectra and are considered as a direct detection of hydrogen bonds. Here, the LBHB model (cf. Figure 1a) involves two electronegative nitrogen atoms, one of which is protonated; thus, there should exist homonuclear hydrogen-bond mediated  $^{15}\text{N}$ – $^{15}\text{N}$   $J$ -couplings ( $^2J(\text{N}_{\delta_1}\cdots\text{H}\cdots$

$\text{N}_{\epsilon_2}$ ) between the two involved nitrogen atoms. In the water-His37 hydrogen bonding model (cf. Figure 1b), the two involved electronegative atoms are nitrogen and oxygen, meaning that there should be heteronuclear hydrogen-bond mediated  $^{15}\text{N}$ – $^{17}\text{O}$   $J$ -couplings between the nitrogen and oxygen, but not homonuclear  $^{15}\text{N}$ – $^{15}\text{N}$   $J$ -couplings. Therefore, we use  $^{15}\text{N}$  2D  $J$ -resolved spectroscopy in high-resolution solid-state NMR to differentiate the hydrogen bonding partners at the heart of the His37 tetrad of the M2FL proton channel.

As demonstrated in the literature,<sup>41</sup> the rotor-synchronized spin-echo (CP –  $t_1/2$  –  $\pi$  –  $t_1/2$  –  $t_2$ ) sequence can be used to measure homonuclear  $J$ -couplings, where CP stands for cross-polarization from  $^1\text{H}$  to  $^{15}\text{N}$ ,  $t_1$  and  $t_2$  represent the time evolution in the indirect and observed dimension, respectively, where  $t_1/2$  has to be set to a multiple of spinning periods. High power  $^1\text{H}$  decoupling is applied during the entire  $t_1$  and  $t_2$  dimensions. Because there are two nitrogen sites in the imidazole ring of histidine separated by two covalent bonds, we need to first examine whether or not there exists a two-bond  $J$ -coupling (i.e.,  $^2J(\text{N}_{\delta_1}\cdots\text{N}_{\epsilon_2})$ ) between these two nitrogen atoms. Figure 2 shows the  $^{15}\text{N}$  2D  $J$ -resolved spectrum for the

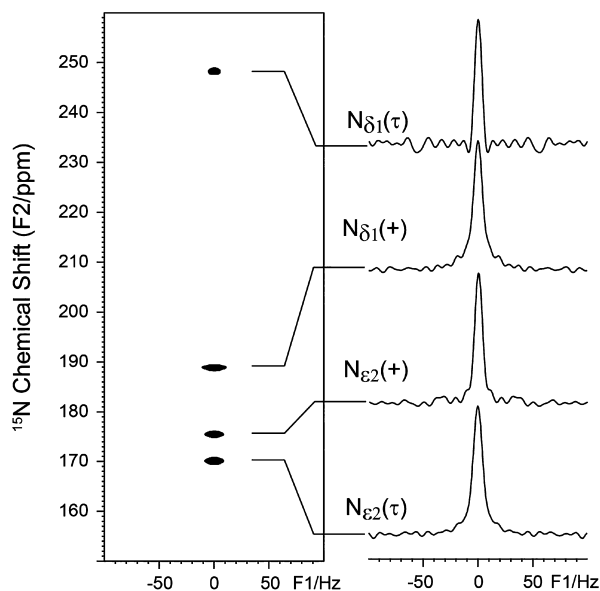


**Figure 2.**  $^{15}\text{N}$  2D  $J$ -resolved spectrum (left) of the histidine powder sample (at pH 6.3) and their corresponding slices (right).

histidine sample lyophilized from a pH 6.3 solution. At this pH, there are two tautomeric states, the neutral  $\tau$  state and the charged state; the  $\pi$  state is not present at this pH.<sup>44</sup> From the slices in the right panel, it is clear that the protonated  $^{15}\text{N}$  sites (especially  $\text{N}_{\epsilon_2}$ ) have a slightly broader line width ( $\sim 9$  Hz) than the nonprotonated  $^{15}\text{N}$  site ( $\sim 7$  Hz), owing to some residual  $^1\text{H}$ – $^{15}\text{N}$  interactions for the protonated  $^{15}\text{N}$  sites that are not fully refocused by the spin echo sequence. Nevertheless, no  $J$ -splitting is observed for the histidine sample, implying that there is no detectable  $^2J(\text{N}_{\delta_1}\cdots\text{N}_{\epsilon_2})$  between the  $\text{N}_{\delta_1}$  and  $\text{N}_{\epsilon_2}$  sites that are separated by two chemical bonds in the imidazole rings for both charged and neutral  $\tau$  states.

Figure S1 shows the  $^{15}\text{N}$  CPMAS NMR spectrum of the His37-labeled M2FL ( $\text{H}_{57,90}\text{Y}$ , pH 6.2) in DOPC/DOPE liposomes. It is noteworthy that, in the uniform  $^{13}\text{C}$  and  $^{15}\text{N}$  labeling media for this protein expression, unlabeled Phe, Tyr,

and Trp amino acids were added to the bacterial cultures to suppress these aromatic amino acid resonances. Therefore, the observed signals from 150 to 260 ppm, as shown in the expanded spectrum in Figure S1 and in refs 26, 31, and 32 are solely from the His37 tetrad. Furthermore, it is important to emphasize that the M2 spectra display a broad distribution of  $^{15}\text{N}$  chemical shifts for both the protonated and nonprotonated  $^{15}\text{N}$  His37 side chain resonances.<sup>26</sup> These resonances have been shown to be heterogeneously and not homogeneously broadened.<sup>26,32</sup> In addition, the heterogeneity largely results from transmembrane helix–helix packing. This proton channel is formed by a tetramer of a single transmembrane helix, and unlike many transmembrane proteins that have small residues at the helix–helix interface, M2 has large side chains, such as Leu38, that can take on different  $\chi_2$  rotameric states resulting in slightly different  $^{15}\text{N}$ – $^{15}\text{N}$  distances for the imidazole-imidazolium hydrogen bonded state leading to the broad distribution of the  $^{15}\text{N}$ ,  $^{13}\text{C}$ , and  $^1\text{H}$  chemical shifts observed for His37.<sup>26,32</sup> Such heterogeneity may be the key to the instability of the imidazole-imidazolium hydrogen bonds that permit proton conductance, albeit on the very slow millisecond time scale. Such a slow time scale is not explained by the mechanism illustrated in Figure 1b.

Figure 3 shows the  $^{15}\text{N}$  2D  $J$ -resolved spectrum of the His37-labeled M2FL protein at pH 6.2 in DOPC/DOPE

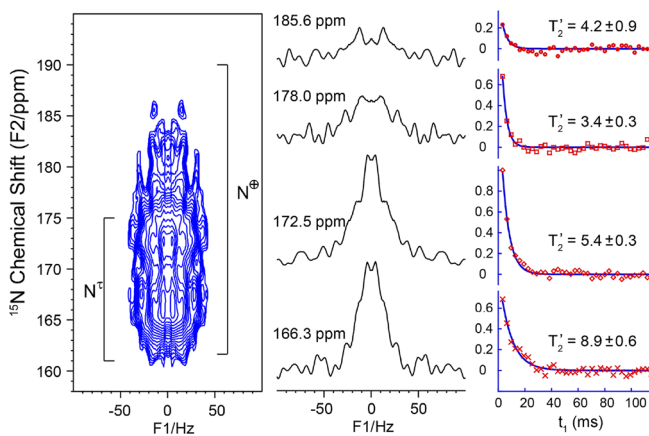


**Figure 3.** Expanded  $^{15}\text{N}$  2D  $J$ -resolved spectrum (left) of the His37-labeled M2FL (pH 6.2) in DOPC/DOPE liposomes and the slices (middle panel) and the normalized echo signal intensities as a function of spin-echo time  $t_1$  (right panel) at different chemical shift positions. This 2D spectrum was recorded in 109 h on a 600 MHz NMR spectrometer where the Larmor frequencies are 600.1 and 60.8 MHz for  $^1\text{H}$  and  $^{15}\text{N}$ , respectively. The sample was spun at 12.5 kHz. The expected protonated  $^{15}\text{N}$  chemical shift range for the  $\tau$  and charge states are marked in the 2D spectrum.

liposomes together with extracted rows at specific  $^{15}\text{N}$  chemical shifts. The natural line width for all  $^{15}\text{N}$  chemical shift positions from 165 to 190 ppm appears to be  $\sim 60$  Hz. This implies, as described above, that the broad  $^{15}\text{N}$  resonance bands observed from 165 to 190 ppm are the result of inhomogeneous broadening, a distribution of chemically distinguishable His37 conformations, rather than exchange broadening at a rate comparable to the chemical shift difference between the protonated and nonprotonated  $\text{N}_{\delta 1}$  and  $\text{N}_{\epsilon 2}$  sites. The slices through the 2D data set (Figure 3) do not have enough sensitivity owing to having just four  $^{15}\text{N}_{\delta 1}$  and four  $^{15}\text{N}_{\epsilon 2}$  sites whose signals are each spread over more than

25 ppm between 160 and 200 ppm in this full length protein in liquid crystalline lipid bilayers. But the transverse dephasing times ( $T'_2$ )<sup>45</sup> from fittings (Figure 3) decrease steadily at a higher ppm position, all shorter than that of the amide nitrogen (Figure S2). Such a decrease in  $T'_2$  could indicate the presence of  $J$ -coupling (eq S1). It is known that the homonuclear  $J$ -coupling can be refocused by applying a  $\pi/2$  pulse in the middle of double spin-echoes (Figure S3).<sup>46,47</sup> Figure 4 shows

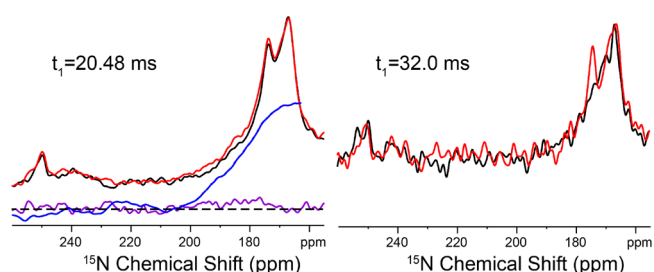


**Figure 4.** Expanded  $^{15}\text{N}$  doubly spin-echoed spectra of the His37-labeled M2FL (pH 6.2) in DOPC/DOPE liposomes with (red) and without (black) the  $J$ -refocusing  $\pi/2$  pulse at different spin-echo time  $t_1$ . The subtraction of the black from red spectra is shown in purple with dashed lines indicating the zero reference. The blue line shows the integration of the difference spectrum from 260 to 164 ppm.

the doubly spin-echoed  $^{15}\text{N}$  spectra of the M2FL sample with and without  $J$ -refocusing. At  $t_1 = 20.48$  ms, the  $J$ -refocused signals (in red) from 170 to 185 ppm are consistently higher than those (in black) without applying the  $\pi/2$  pulse, as clearly indicated by the integration curve (blue). These results document the existence of  $^2\text{h}J(\text{N}_{\delta 1}\cdots\text{H}\cdots\text{N}_{\epsilon 2})$  as suggested previously through the  $^{15}\text{N}$ – $^1\text{H}$  correlation spectra with  $^1\text{H}$  frequencies up to 18.7 ppm and  $^{15}\text{N}$  frequencies up to 195 ppm.<sup>26</sup> Using  $t_1 = 32.0$  ms, the  $J$ -refocused signal at 174 ppm had a much higher intensity (above the noise level) than without the  $J$ -refocusing, whose ratio yielded a  $^2\text{h}J(\text{N}_{\delta 1}\cdots\text{H}\cdots\text{N}_{\epsilon 2})$  value of 8.1 Hz from eqs S1 and S2, which represents typical  $^2\text{h}J(\text{N}\cdots\text{H}\cdots\text{N})$  values observed in other compounds.<sup>41–43</sup> This confirms the existence of imidazole-imidazolium hydrogen bonds in the His37 tetrad of the M2 protein, since the control spectrum (Figure 2) indicates no two-bond  $J$ -coupling between the  $\text{N}_{\delta 1}$  and  $\text{N}_{\epsilon 2}$  sites within the imidazole ring. The further decrease in the  $T'_2$  values at the higher  $^{15}\text{N}$  chemical shifts might indicate a larger  $^2\text{h}J(\text{N}_{\delta 1}\cdots\text{H}\cdots\text{N}_{\epsilon 2})$  and thus could imply stronger hydrogen bonds as the protonated  $^{15}\text{N}$  chemical shift moves to lower field.<sup>26,32</sup> Thus, the large  $^2\text{h}J(\text{N}_{\delta 1}\cdots\text{H}\cdots\text{N}_{\epsilon 2})$  values hypothesized here are consistent with the observation of high  $^1\text{H}$  and  $^{15}\text{N}$  chemical shifts observed in the  $^1\text{H}$ – $^{15}\text{N}$  HETCOR spectra for the same sites, all reflecting on the broad range of the imidazole-imidazolium hydrogen-bond strengths in the His37 tetrad.<sup>26,30,32</sup> These relatively infrequent strong hydrogen bonds may be responsible for the low M2 proton conductance rate. Furthermore, this range of  $J$ -couplings and chemical shifts is consistent with the explanation that packing of various large hydrophobic side chains in the helix–helix interface results in a subtle range of distances between the imidazole and imidazolium side chains due to slight shifts in the  $\text{C}\alpha$ – $\text{C}\alpha$  separation of the backbone.<sup>26</sup>

To conclude, we used the 2D  $J$ -resolved NMR spectrum to measure the hydrogen-bond mediated  $^{15}\text{N}$ – $^{15}\text{N}$   $J$ -couplings at the heart of the His37 tetrad of the M2 protein. The observed  $^2\text{h}J(\text{N}_{\delta 1}\cdots\text{H}\cdots\text{N}_{\epsilon 2})$  provides direct observation of the heteroge-



neous imidazole-imidazolium hydrogen bonds in the His37 tetrad of the M2 protein, thus validating the LBHB proton conduction mechanism at the heart of the M2FL proton channel. Furthermore, these *J*-couplings are highly correlated with distributions of chemical shifts, as in disordered solids,<sup>48,49</sup> and could be used to refine detailed local structural models in such heterogeneous environments through theoretical calculations.<sup>35,50</sup>

## ■ ASSOCIATED CONTENT

### Supporting Information

The Supporting Information is available free of charge at <https://pubs.acs.org/doi/10.1021/jacs.9b09985>.

Materials and experimental details; 1D <sup>15</sup>N CPMAS spectrum of the His37-labeled M2FL sample; 1D spectra taken along the F1 dimension of the 2D *J*-resolved spectrum in Figure 3; demonstration for the double spin-echo sequence used for *J*-refocusing and the full doubly spin-echoed spectra of the M2FL sample at different echo times (PDF)

## ■ AUTHOR INFORMATION

### Corresponding Author

Riqiang Fu – National High Magnet Field Lab, Tallahassee, Florida 32310, United States; [orcid.org/0000-0003-0075-0410](https://orcid.org/0000-0003-0075-0410); Email: [rfu@magnet.fsu.edu](mailto:rfu@magnet.fsu.edu)

### Authors

Yimin Miao – Department of Chemistry and Biochemistry, Florida State University, Tallahassee, Florida 32306, United States

Huajun Qin – Department of Chemistry and Biochemistry, Florida State University, Tallahassee, Florida 32306, United States

Timothy A. Cross – National High Magnet Field Lab, Tallahassee, Florida 32310, United States; Department of Chemistry and Biochemistry, Florida State University, Tallahassee, Florida 32306, United States

Complete contact information is available at: <https://pubs.acs.org/doi/10.1021/jacs.9b09985>

### Notes

The authors declare no competing financial interest.

## ■ ACKNOWLEDGMENTS

This work was supported by NIH Grants AI023007 and AI119178. All NMR experiments were carried out at the National High Magnetic Field Lab (NHMFL) supported by the NSF Cooperative Agreement DMR-1644779 and the State of Florida.

## ■ REFERENCES

(1) Sugrue, R. J.; Hay, A. J. Structural characteristics of the M2 protein of influenza-A viruses - evidence that it forms a tetrameric channel. *Virology* **1991**, *180*, 617.

(2) Sakaguchi, T.; Tu, Q. A.; Pinto, L. H.; Lamb, R. A. The active oligomeric state of the minimalistic influenza virus M-2 ion channel is a tetramer. *Proc. Natl. Acad. Sci. U. S. A.* **1997**, *94*, 5000.

(3) Hu, J.; Asbury, T.; Achuthan, S.; Li, C.; Bertram, R.; Quine, J. R.; Fu, R.; Cross, T. A. Backbone structure of the amantadine-blocked trans-membrane domain M2 proton channel from influenza A virus. *Biophys. J.* **2007**, *92*, 4335.

(4) Nishimura, K.; Kim, S. G.; Zhang, L.; Cross, T. A. The closed state of a H<sup>+</sup> channel helical bundle combining precise orientational and distance restraints from solid state NMR. *Biochemistry* **2002**, *41*, 13170.

(5) Lamb, R. A.; Zebedee, S. L.; Richardson, C. D. Influenza virus-M2 protein is an integral membrane-protein expressed on the infected-cell surface. *Cell* **1985**, *40*, 627.

(6) Grambas, S.; Bennett, M. S.; Hay, A. J. Influence of amantadine resistance mutations on the pH regulatory function of the M2-protein of influenza-A viruses. *Virology* **1992**, *191*, 541.

(7) Hu, J.; Fu, R.; Nishimura, K.; Zhang, L.; Zhou, H. X.; Busath, D. D.; Vijayvergiya, V.; Cross, T. A. Histidines, heart of the hydrogen ion channel from influenza A virus: Toward an understanding of conductance and proton selectivity. *Proc. Natl. Acad. Sci. U. S. A.* **2006**, *103*, 6865.

(8) Miao, Y.; Qin, H.; Fu, R.; Sharma, M.; Can, T. V.; Hung, I.; Luca, S.; Gor'kov, P. L.; Brey, W. W.; Cross, T. A. M2 Proton Channel Structural Validation from Full-Length Protein Samples in Synthetic Bilayers and *E. coli* Membranes. *Angew. Chem.* **2012**, *124*, 8508.

(9) Can, T. V.; Sharma, M.; Hung, I.; Gor'kov, P. L.; Brey, W. W.; Cross, T. A. Magic Angle Spinning and Oriented Sample Solid-State NMR Structural Restraints Combine for Influenza A M2 Protein Functional Insights. *J. Am. Chem. Soc.* **2012**, *134*, 9022.

(10) Cady, S. D.; Schmidt-Rohr, K.; Wang, J.; Soto, C. S.; DeGrado, W. F.; Hong, M. Structure of the amantadine binding site of influenza M2 proton channels in lipid bilayers. *Nature* **2010**, *463*, 689.

(11) Cady, S. D.; Mishanina, T. V.; Hong, M. Structure of amantadine-bound M2 transmembrane peptide of influenza A in lipid bilayers from magic-angle-spinning solid-state NMR: the role of Ser31 in amantadine binding. *J. Mol. Biol.* **2009**, *385*, 1127.

(12) Andreas, L. B.; Eddy, M. T.; Pielak, R. M.; Chou, J. J.; Griffin, R. G. Magic angle spinning NMR investigation of Influenza A M2<sub>18–60</sub>: Support for an allosteric mechanism of inhibition. *J. Am. Chem. Soc.* **2010**, *132*, 10958.

(13) Andreas, L. B.; Eddy, M. T.; Chou, J. J.; Griffin, R. G. Magic-angle-spinning NMR of the drug resistant S31N M2 proton transporter from Influenza A. *J. Am. Chem. Soc.* **2012**, *134*, 7215.

(14) Colvin, M. T.; Andreas, L. B.; Chou, J. J.; Griffin, R. G. Proton association constants of His 37 in the Influenza-A M218–60 dimer-of-dimers. *Biochemistry* **2014**, *53*, 5987.

(15) Andreas, L. B.; Reese, M.; Eddy, M. T.; Gelev, V.; Ni, Q. Z.; Miller, E. A.; Emsley, L.; Pintacuda, G.; Chou, J. J.; Griffin, R. G. Structure and mechanism of the Influenza A M218–60 Dimer of Dimers. *J. Am. Chem. Soc.* **2015**, *137*, 14877.

(16) Du, J.; Cross, T. A.; Zhou, H. X. Recent progress in structure-based anti-influenza drug design. *Drug Discovery Today* **2012**, *17*, 1111.

(17) Sharma, M.; Yi, M.; Dong, H.; Qin, H.; Peterson, E.; Busath, D. D.; Zhou, H. X.; Cross, T. A. Insight into the mechanism of the influenza A proton channel from a structure in a lipid bilayer. *Science* **2010**, *330*, 509.

(18) Wang, J.; Wu, Y.; Ma, C.; Fiorin, G.; Wang, J.; Pinto, L. H.; Lamb, R. A.; Klein, M. L.; DeGrado, W. F. Structure and inhibition of the drug-resistant S31N mutant of the M2 ion channel of influenza A virus. *Proc. Natl. Acad. Sci. U. S. A.* **2013**, *110*, 1315.

(19) Wang, J. F.; Kim, S. G.; Kovacs, F.; Cross, T. A. Structure of the transmembrane region of the M2 protein H<sup>+</sup> channel. *Protein Sci.* **2001**, *10*, 2241.

(20) Schnell, J. R.; Chou, J. J. Structure and mechanism of the M2 proton channel of influenza A virus. *Nature* **2008**, *451*, 591.

(21) Pielak, R. M.; Schnell, J. R.; Chou, J. J. Mechanism of drug inhibition and drug resistance of influenza A M2 channel. *Proc. Natl. Acad. Sci. U. S. A.* **2009**, *106*, 7379.

(22) Pielak, R. M.; Oxenoid, K.; Chou, J. J. Structural investigation of rimantadine inhibition of the AM2-BM2 chimera channel of influenza viruses. *Structure* **2011**, *19*, 1655.

- (23) Pielak, R. M.; Chou, J. J. Solution NMR structure of the V27A drug resistant mutant of influenza A M2 channel. *Biochem. Biophys. Res. Commun.* **2010**, *401*, 58.
- (24) Stouffer, A. L.; Acharya, R.; Salom, D.; Levine, A. S.; Di Costanzo, L.; Soto, C. S.; Tereshko, V.; Nanda, V.; Stayrook, S.; DeGrado, W. F. Structural basis for the function and inhibition of an influenza virus proton channel. *Nature* **2008**, *451*, 596.
- (25) Acharya, R.; Carnevale, V.; Fiorin, G.; Levine, B. G.; Polishchuk, A. L.; Balannik, V.; Samish, I.; Lamb, R. A.; Pinto, L. H.; DeGrado, W. F.; Klein, M. L. Structure and mechanism of proton transport through the transmembrane tetrameric M2 protein bundle of the influenza A virus. *Proc. Natl. Acad. Sci. U. S. A.* **2010**, *107*, 15075.
- (26) Miao, Y.; Fu, R.; Zhou, H. X.; Cross, T. A. Dynamic short hydrogen bonds in histidine tetrad of full length M2 proton channel reveal tetrameric structural heterogeneity and functional mechanism. *Structure* **2015**, *23*, 2300.
- (27) Hu, F.; Schmidt-Rohr, K.; Hong, M. NMR Detection of pH-Dependent Histidine-Water Proton Exchange Reveals the Conduction Mechanism of a Transmembrane Proton Channel. *J. Am. Chem. Soc.* **2012**, *134*, 3703.
- (28) Hong, M.; Fritzsche, K. J.; Williams, J. K. Hydrogen-Bonding Partner of the Proton-Conducting Histidine in the Influenza M2 Proton Channel Revealed From  $^1\text{H}$  Chemical Shifts. *J. Am. Chem. Soc.* **2012**, *134*, 14753.
- (29) Liang, R.; Li, H.; Swanson, J. M. J.; Voth, G. A. Multiscale simulation reveals a multifaceted mechanism of proton permeation through the influenza A M2 proton channel. *Proc. Natl. Acad. Sci. U. S. A.* **2014**, *111*, 9396.
- (30) Eckert, H.; Yesinowski, J. P.; Silver, L. A.; Stolper, E. M. Water in silicate glasses: Quantitation and structural studies by proton solid echo and magic angle spinning NMR methods. *J. Phys. Chem.* **1988**, *92*, 2055.
- (31) Fu, R.; Miao, Y.; Qin, H.; Cross, T. A. Probing Hydronium Ion Histidine NH Exchange Rate Constants in the M2 Channel via Indirect Observation of Dipolar-Dephased  $^{15}\text{N}$  Signals in Solid-State Magic-Angle-Spinning NMR. *J. Am. Chem. Soc.* **2016**, *138*, 15801.
- (32) Qin, H.; Miao, Y.; Cross, T. A.; Fu, R. Beyond structural biology to functional biology: Solid-state NMR experiments and strategies for understanding the M2 proton channel conductance. *J. Phys. Chem. B* **2017**, *121*, 4799.
- (33) Grabowski, S. J. What Is the Covalency of Hydrogen Bonding? *Chem. Rev.* **2011**, *111*, 2597.
- (34) Dingley, A. J.; Cordier, F.; Grzesiek, S. An Introduction to Hydrogen Bond Scalar Couplings. *Concepts Magn. Reson.* **2001**, *13*, 103.
- (35) Joyce, S. A.; Yates, J. R.; Pickard, C. J.; Brown, S. P. Density Functional Theory Calculations of Hydrogen-Bond-Mediated NMR J Coupling in the Solid State. *J. Am. Chem. Soc.* **2008**, *130*, 12663.
- (36) Blake, J. B.; Adams, M. W. W.; Summers, M. F. Novel Observation of NH-S(Cys) Hydrogen-Bond-Mediated Scalar Coupling in  $^{113}\text{Cd}$ -Substituted Rubredoxin from *Pyrococcus furiosus*. *J. Am. Chem. Soc.* **1992**, *114*, 4931.
- (37) Dingley, A. J.; Grzesiek, S. Direct observation of hydrogen bonds in nucleic acid base pairs by internucleotide  $^2\text{J}_{\text{NN}}$  couplings. *J. Am. Chem. Soc.* **1998**, *120*, 8293.
- (38) Pervushin, K.; Ono, A.; Fernandez, C.; Szyperski, T.; Kainosho, M.; Wuthrich, K. NMR scalar couplings across Watson/Crick base pair hydrogen bonds in DNA observed by transverse relaxation-optimized spectroscopy. *Proc. Natl. Acad. Sci. U. S. A.* **1998**, *95*, 14147.
- (39) Cornilescu, G.; Hu, J. S.; Bax, A. Identification of the hydrogen bonding network in a protein by scalar couplings. *J. Am. Chem. Soc.* **1999**, *121*, 2949.
- (40) Hennig, M.; Geierstanger, B. H. Direct detection of a histidine-histidine side chain hydrogen bond important for folding of apomyoglobin. *J. Am. Chem. Soc.* **1999**, *121*, 5123.
- (41) Brown, S. P.; Perez-Torralba, M.; Sanz, D.; Claramunt, R. M.; Emsley, L. Determining hydrogen-bond strengths in the solid state by NMR: the quantitative measurement of homonuclear J couplings. *Chem. Commun.* **2002**, 1852.
- (42) Brown, S. P.; Perez-Torralba, M.; Sanz, D.; Claramunt, R. M.; Emsley, L. The Direct Detection of a Hydrogen Bond in the Solid State by NMR through the Observation of a Hydrogen-Bond Mediated  $^{15}\text{N}$ - $^{15}\text{N}$  J Coupling. *J. Am. Chem. Soc.* **2002**, *124*, 1152.
- (43) Pham, T. N.; Griffin, J. M.; Masiero, S.; Lena, S.; Gottarelli, G.; Hodgkinson, P.; Filip, C.; Brown, S. P. Quantifying hydrogen-bonding strength: the measurement of  $^2\text{J}_{\text{NN}}$  couplings in self-assembled guanosines by solid-state  $^{15}\text{N}$  spin-echo MAS NMR. *Phys. Chem. Chem. Phys.* **2007**, *9*, 3416.
- (44) Miao, Y.; Cross, T. A.; Fu, R. Differentiation of histidine tautomeric states using  $^{15}\text{N}$  selectively filtered  $^{13}\text{C}$  solid-state NMR spectroscopy. *J. Magn. Reson.* **2014**, *245*, 105.
- (45) Lesage, A.; Emsley, L.; Penin, F.; Bockmann, A. Investigation of Dipolar-Mediated Water-Protein Interactions in Microcrystalline Crh by Solid-State NMR Spectroscopy. *J. Am. Chem. Soc.* **2006**, *128*, 8246.
- (46) Takegoshi, K.; Ogura, K.; Hikichi, K. A Perfect Spin Echo in a Weakly Homonuclear J-Coupled Two Spin-1/2 System. *J. Magn. Reson.* **1989**, *84*, 611.
- (47) van Zijl, P. C. M.; Moonen, C. T. W.; von Kienlin, M. Homonuclear J refocusing in Echo Spectroscopy. *J. Magn. Reson.* **1990**, *89*, 28.
- (48) Cadars, S.; Lesage, A.; Trierweiler, M.; Heux, L.; Emsley, L. NMR measurements of scalar-coupling distributions in disordered solids. *Phys. Chem. Chem. Phys.* **2007**, *9*, 92.
- (49) Guerry, P.; Smith, M. E.; Brown, S. P.  $^{31}\text{P}$  MAS Refocused INADEQUATE Spin-Echo (REINE) NMR Spectroscopy: Revealing J Coupling and Chemical Shift Two-Dimensional Correlations in Disordered Solids. *J. Am. Chem. Soc.* **2009**, *131*, 11861.
- (50) Hughes, C. E.; Reddy, G. N. M.; Masiero, S.; Brown, S. P.; Williams, P. A.; Harris, K. D. M. Determination of a complex crystal structure in the absence of single crystals: analysis of powder X-ray diffraction data, guided by solid-state NMR and periodic DFT calculations, reveals a new 2'-deoxyguanosine structural motif. *Chem. Sci.* **2017**, *8*, 3971.